Supplementary information: A mammalian circadian clock model incorporating daytime expression elements

Craig C. Jolley, Maki Ukai-Tadenuma, Dimitri Perrin, Hiroki R. Ueda

Supplementary Methods

Derivation of dimensionless model equations

We begin by writing our model equations in a conventional format (1):

$$\begin{aligned}
\frac{da}{dt} &= \beta_{ma} h_1(C) - \alpha_{ma} a & \frac{dA}{dt} &= \beta_{pA} a - \alpha_{pA} A \\
\frac{db}{dt} &= \beta_{mb} g_{2,3}(A,E) - \alpha_{mb} b & \frac{dB}{dt} &= \beta_{pB} b - \alpha_{pB} B \\
\frac{dc}{dt} &= \beta_{mc}\left(g_{4,7}(A,E) + g_{5,6}(B,D)\right) - \alpha_{mc} c & \frac{dC}{dt} &= \beta_{pC} c - \alpha_{pC} C \\
\frac{dd}{dt} &= \beta_{md} h_8(C) - \alpha_{md} d & \frac{dD}{dt} &= \beta_{pD} d - \alpha_{pD} D \\
\frac{de}{dt} &= \beta_{me} g_{9,10}(B,D) - \alpha_{me} e & \frac{dE}{dt} &= \beta_{pE} e - \alpha_{pE} E
\end{aligned} \qquad \text{(S1)}$$

Where {*a*..*e*} represent mRNA concentrations, {*A*..*E*} represent protein concentrations, {α_{mx}, α_{pX}} represent degradation rates, and {β_{mx}, β_{pX}} represent synthesis rates. The functions $h(R)$ and $g(A,R)$ are used to capture the effects of gene regulation; both are bounded to the interval [0,1], with $h(R)$ monotonically decreasing (repression), and $g(A,R)$ increasing in A but decreasing in R (activation and repression on the same promoter). Binding follows the Hill equation; activators and repressors bind competitively to the same promoter:

$$h_i(R) = \frac{1}{1 + \left(R/k_i\right)^n} \qquad g_{i,j}(A,R) = \frac{\left(A/k_i\right)^n}{1 + \left(A/k_i\right)^n + \left(R/k_j\right)^n} \qquad \text{(S2)}$$

Here, k_i is the binding constant for binding reaction i. To limit the number of free parameters, the Hill coefficient n was assumed to be equal for all reactions.

To non-dimensionalize these equations, we will need to make the following substitutions:

$$\begin{aligned} a &\to a_c \tilde{a} \\ A &\to A_c \tilde{A}, \\ t &\to t_c \tau \end{aligned} \tag{S3}$$

so that dimensional quantities, such as the concentration *a*, are replaced by a constant scale a_c with units of concentration and a unitless parameter $\tilde{a}$. Now our dynamical equations are:

$$\frac{d\tilde{a}}{d\tau} = \frac{\beta_{ma} t_c}{a_c} h_1\left(C_c \tilde{C}\right) - \alpha_{ma} t_c \tilde{a} \qquad \frac{d\tilde{A}}{d\tau} = \frac{\beta_{pA} a_c t_c}{A_c} \tilde{a} - \alpha_{pA} t_c \tilde{A}$$

$$\frac{d\tilde{b}}{d\tau} = \frac{\beta_{mb} t_c}{b_c} g_{2,3}\left(A_c \tilde{A}, E_c \tilde{E}\right) - \alpha_{mb} t_c \tilde{b} \qquad \frac{d\tilde{B}}{d\tau} = \frac{\beta_{pB} b_c t_c}{B_c} \tilde{b} - \alpha_{pB} t_c \tilde{B}$$

$$\frac{d\tilde{c}}{d\tau} = \frac{\beta_{mc} t_c}{c_c}\left(g_{4,7}\left(A_c \tilde{A}, E_c \tilde{E}\right) + g_{5,6}\left(B_c \tilde{B}, D_c \tilde{D}\right)\right) - \alpha_{mc} t_c \tilde{c} \qquad \frac{d\tilde{C}}{d\tau} = \frac{\beta_{pC} c_c t_c}{C_c} \tilde{c} - \alpha_{pC} t_c \tilde{C}$$

$$\frac{d\tilde{d}}{d\tau} = \frac{\beta_{md} t_c}{d_c} h_8\left(C_c \tilde{C}\right) - \alpha_{md} t_c \tilde{d} \qquad \frac{d\tilde{D}}{d\tau} = \frac{\beta_{pD} d_c t_c}{D_c} \tilde{d} - \alpha_{pD} t_c \tilde{D}$$

$$\frac{d\tilde{e}}{d\tau} = \frac{\beta_{me} t_c}{e_c} g_{9,10}\left(B_c \tilde{B}, D_c \tilde{D}\right) - \alpha_{me} t_c \tilde{e} \qquad \frac{d\tilde{E}}{d\tau} = \frac{\beta_{pE} e_c t_c}{E_c} \tilde{e} - \alpha_{pE} t_c \tilde{E}$$

Now define the characteristic mRNA concentrations and dimensionless decay constants as:

$$\begin{aligned} a_c &= t_c \beta_{ma}, \text{ etc.} \\ \eta_{ma} &= t_c \alpha_{ma}, \text{ etc.} \end{aligned} \tag{S4}$$

The model equations now become:

$$\begin{aligned}
\frac{d\tilde{a}}{d\tau} &= h_1\left(C_c\tilde{C}\right)-\eta_{ma}\tilde{a} & \frac{d\tilde{A}}{d\tau} &= \frac{\beta_{pA}\beta_{ma}{t_c}^2}{A_c}\tilde{a}-\eta_{pA}\tilde{A}\\
\frac{d\tilde{b}}{d\tau} &= g_{2,3}\left(A_c\tilde{A},E_c\tilde{E}\right)-\eta_{mb}\tilde{b} & \frac{d\tilde{B}}{d\tau} &= \frac{\beta_{pB}\beta_{mb}{t_c}^2}{B_c}\tilde{b}-\eta_{pB}\tilde{B}\\
\frac{d\tilde{c}}{d\tau} &= \left(g_{4,7}\left(A_c\tilde{A},E_c\tilde{E}\right)+g_{5,6}\left(B_c\tilde{B},D_c\tilde{D}\right)\right)-\eta_{mc}\tilde{c} & \frac{d\tilde{C}}{d\tau} &= \frac{\beta_{pC}\beta_{mc}{t_c}^2}{C_c}\tilde{c}-\eta_{pC}\tilde{C}\\
\frac{d\tilde{d}}{d\tau} &= h_8\left(C_c\tilde{C}\right)-\eta_{md}\tilde{d} & \frac{d\tilde{D}}{d\tau} &= \frac{\beta_{pD}\beta_{md}{t_c}^2}{D_c}\tilde{d}-\eta_{pD}\tilde{D}\\
\frac{d\tilde{e}}{d\tau} &= g_{9,10}\left(B_c\tilde{B},D_c\tilde{D}\right)-\eta_{me}\tilde{e} & \frac{d\tilde{E}}{d\tau} &= \frac{\beta_{pE}\beta_{me}{t_c}^2}{E_c}\tilde{e}-\eta_{pE}\tilde{E}
\end{aligned} \qquad \text{(S5)}$$

Now we can define characteristic protein concentrations:

$$A_c = {t_c}^2\beta_{ma}\beta_{pA} \qquad \text{(S6)}$$

Also, our activation functions (**Eq. S2**) can be replaced by

$$H_i\left(\tilde{R}\right)=\frac{1}{1+\left(\chi_i\tilde{R}\right)^n} \qquad g_{i,j}\left(\tilde{A},\tilde{R}\right)=\frac{\left(\chi_i\tilde{A}\right)^n}{1+\left(\chi_i\tilde{A}\right)^n+\left(\chi_j\tilde{R}\right)^n} \qquad \text{(S7)}$$

Where

$\chi_1=\frac{{t_c}^2\beta_{mc}\beta_{pC}}{k_1}$, etc. are dimensionless activation/repression parameters.

Finally, our dimensionless model equations are:

$$\begin{aligned}
\frac{d\tilde{a}}{d\tau} &= \tilde{h}_1\left(\tilde{C}\right)-\eta_{ma}\tilde{a} & \frac{d\tilde{A}}{d\tau} &= \tilde{a}-\eta_{pA}\tilde{A}\\
\frac{d\tilde{b}}{d\tau} &= \tilde{g}_{2,3}\left(\tilde{A},\tilde{E}\right)-\eta_{mb}\tilde{b} & \frac{d\tilde{B}}{d\tau} &= \tilde{b}-\eta_{pB}\tilde{B}\\
\frac{d\tilde{c}}{d\tau} &= \left(\tilde{g}_{4,7}\left(\tilde{A},\tilde{E}\right)+\tilde{g}_{5,6}\left(\tilde{B},\tilde{D}\right)\right)-\eta_{mc}\tilde{c} & \frac{d\tilde{C}}{d\tau} &= \tilde{c}-\eta_{pC}\tilde{C}\\
\frac{d\tilde{d}}{d\tau} &= \tilde{h}_8\left(\tilde{C}\right)-\eta_{md}\tilde{d} & \frac{d\tilde{D}}{d\tau} &= \tilde{d}-\eta_{pD}\tilde{D}\\
\frac{d\tilde{e}}{d\tau} &= \tilde{g}_{9,10}\left(\tilde{B},\tilde{D}\right)-\eta_{me}\tilde{e} & \frac{d\tilde{E}}{d\tau} &= \tilde{e}-\eta_{pE}\tilde{E}
\end{aligned} \qquad \text{(S8)}$$

The tildes are now superfluous, as all quantities are dimensionless. We have reduced the number of explicit parameters from 31 to 21. The remaining 10 parameters account for (arbitrary) rescaling of model variables to produce output with units of concentration.

Estimating mRNA-protein phase lags

Due to the lack of accurate quantitative data on protein oscillation phases, mRNA-protein phase lags were estimated based on estimates of the protein amplitude. It should be noted that this is a model of the SCN clock and protein measurements have generally been restricted to peripheral tissues such as the liver, so even estimates of protein oscillation amplitude should be made cautiously. Beginning with the equation for mRNA concentration,

$$\dot{m} = \frac{1}{2}\left(\cos\omega_0 t + 1\right)\beta_m - \alpha_m m \tag{S9}$$

We can take the Laplace transform:

$$m(t) \xrightarrow{\mathcal{L}} M(s)$$

$$sM(s) = \frac{\beta_m}{2}\frac{s}{s^2 + {\omega_0}^2} + \frac{\beta_m}{2s} - \alpha_m M$$

$$\begin{aligned} M(s) &= \frac{\beta_m}{2}\frac{s}{\left(s^2 + {\omega_0}^2\right)\left(s + \alpha_m\right)} + \frac{\beta_m}{2}\frac{1}{s\left(s + \alpha_m\right)} \\ &= \frac{\beta_m}{2}\left(\frac{\alpha_m s + \omega_0^2}{\left({\alpha_m}^2 + {\omega_0}^2\right)\left(s^2 + {\omega_0}^2\right)} - \frac{\alpha_m}{\left({\alpha_m}^2 + {\omega_0}^2\right)\left(s + \alpha_m\right)}\right) + \frac{\beta_m}{2\alpha_m}\left(\frac{1}{s} - \frac{1}{s + \alpha_m}\right) \end{aligned} \tag{S10}$$

If we define

$$\phi = \tan^{-1}\frac{\omega_0}{\alpha_m}, \quad \cos\phi = \frac{\alpha_m}{\sqrt{\omega_0^2 + \alpha_m^2}}, \quad \sin\phi = \frac{\omega_0}{\sqrt{\omega_0^2 + \alpha_m^2}} \tag{S11}$$

then

$$\begin{aligned} M(s) &= \frac{\beta_m}{2\sqrt{\omega^2 + \alpha_m^2}}\left(\frac{s\cos\phi + \omega_0\sin\phi}{s^2 + \omega_0^2} - \frac{\alpha_m}{\sqrt{\omega_0^2 + \alpha_m^2}}\frac{1}{s + \alpha_m}\right) + \frac{\beta_m}{2\alpha_m}\left(\frac{1}{s} - \frac{1}{s + \alpha_m}\right) \\ &= \frac{\beta_m}{2\alpha_m}\cos\phi\left(\frac{s\cos\phi + \omega_0\sin\phi}{s^2 + \omega_0^2}\right) - \frac{\beta_m}{2\alpha_m}\cos^2\phi\frac{1}{s + \alpha_m} + \frac{\beta_m}{2\alpha_m}\left(\frac{1}{s} - \frac{1}{s + \alpha_m}\right) \end{aligned} . \tag{S12}$$

We can now take the inverse Laplace transform:

$$M(s) \xrightarrow{\mathcal{L}^{-1}} m(t)$$
$$m(t) = \frac{\beta_m}{2\alpha_m}\cos\phi\cos(\omega_0 t - \phi) - \frac{\beta_m}{2\alpha_m}\left(\cos^2\phi + 1\right)e^{-\alpha_m t} + \frac{\beta_m}{2\alpha_m} \tag{S13}$$
$$\lim_{t\to\infty} m(t) = \frac{\beta_m}{2\alpha_m}\cos\phi\cos(\omega_0 t - \phi) + \frac{\beta_m}{2\alpha_m} \equiv m_\infty(t)$$

If the steady-state solution $m_\infty(t)$ is substituted into Equation S9, the result is equal to the derivative of $m_\infty(t)$, indicating that this solution is valid for all parameter values. The protein case described below is somewhat more complicated.

The solution for the protein term begins with the differential equation:

$$\dot{p} = \beta_p m - \alpha_p p\,, \tag{S14}$$

which we will again solve using a Laplace transform.

$$p(t) \xrightarrow{\mathcal{L}} P(s)$$
$$sP(s) = \beta_p M(s) - \alpha_p P(s) \tag{S15}$$

Rather than inserting the complete solution for $M(s)$, we will omit the initial transient:

$$m_\infty(t) \xrightarrow{\mathcal{L}} M_\infty(s)$$
$$M_\infty(s) = \frac{\beta_m}{2\alpha_m}\cos\phi\left(\frac{s\cos\phi + \omega_0\sin\phi}{s^2 + \omega_0^2}\right) + \frac{\beta_m}{2\alpha_m s} \tag{S16}$$

This will give us the correct long-term behavior for p:

$$\begin{aligned} P(s) &= \frac{\beta_p M(s)}{s + \alpha_p} \approx \frac{\beta_p M_\infty(s)}{s + \alpha_p} \\ &= \frac{\beta_p\beta_m}{2\alpha_m}\cos\phi\,\frac{s\cos\phi + \omega_0\sin\phi}{\left(s^2 + \omega_0^2\right)(s + \alpha_p)} + \frac{\beta_p\beta_m}{2\alpha_m s}\,\frac{1}{s + \alpha_p} \\ &= \frac{\beta_p\beta_m}{2\alpha_m}\,\frac{\cos\phi}{\sqrt{\alpha_p^2 + \omega_0^2}}\left(\frac{s\cos\psi + \omega_0\sin\psi}{s^2 + \omega_0^2} - \frac{\cos\psi}{s + \alpha_p}\right) + \frac{\beta_p\beta_m}{2\alpha_p\alpha_m}\left(\frac{1}{s} - \frac{1}{s + \alpha_p}\right) \end{aligned} \tag{S17}$$

where

$$\psi = \tan^{-1}\left(\frac{\alpha_p\sin\phi + \omega_0\cos\phi}{\alpha_p\cos\phi - \omega_0\sin\phi}\right). \tag{S18}$$

Taking the inverse Laplace transform,

$$P(s) \xrightarrow{\mathcal{L}^{-1}} p(t)$$

$$p(t) = \frac{\beta_p \beta_m}{2\alpha_m} \frac{\cos\phi}{\sqrt{\alpha_p^2 + \omega_0^2}} \left(\cos(\omega_0 t - \psi) - e^{-\alpha_p t} \cos\psi\right) + \frac{\beta_p \beta_m}{2\alpha_p \alpha_m} \left(1 - e^{-\alpha_p t}\right) \tag{S19}$$

$$\lim_{t\to\infty} p(t) = \frac{\beta_p \beta_m}{2\alpha_m} \frac{\cos\phi}{\sqrt{\alpha_p^2 + \omega_0^2}} \cos(\omega_0 t - \psi) + \frac{\beta_p \beta_m}{2\alpha_p \alpha_m}$$

Note that, while the sine and cosine functions have a periodicity of 2π, the period of the tangent function is only π – this means that a phase obtained using the arctangent (as in Equation S18) may need to be shifted by π. To check for this possibility, we can compare the derivative of Equation S19 with a derivative calculated using Equation S14; in general they will only match for the correct value of φ. Checking at a single time point is sufficient; the calculation is simple for $t = 0$:

$$\dot{p}(0) = \frac{d}{dt} p_\infty(0) = \beta_p m_\infty(0) - \alpha_p p_\infty(0)$$

$$= \frac{\omega_0 \beta_m \beta_p}{2\alpha_m} \frac{\cos\phi \sin\psi}{\sqrt{\alpha_p^2 + \omega_0^2}} = \frac{\beta_m \beta_p}{2\alpha_m} \left(\cos^2\phi - \frac{\alpha_p}{\sqrt{\alpha_p^2 + \omega_0^2}} \cos\phi \cos\psi \right) \tag{S20}$$

$$\frac{\omega_0 \sin\psi}{\sqrt{\alpha_p^2 + \omega_0^2}} = \cos\phi - \frac{\alpha_p}{\sqrt{\alpha_p^2 + \omega_0^2}} \cos\psi$$

When φ and ψ are calculated for realistic values of α_p and α_m (as in **Figure S2**), it is often the case that this equality holds for $\psi+\pi$ but not for ψ; ψ must then be adjusted accordingly.

We can now obtain the relative protein oscillation amplitude:

$$A_p = \frac{\alpha_m \alpha_p}{\sqrt{\left(\alpha_p^2 + \omega_0^2\right)\left(\omega_0^2 + \alpha_m^2\right)}} \tag{S21}$$

as well as the phase lag

$$\psi - \phi = \tan^{-1}\left(\frac{\alpha_p \sin\phi + \omega_0 \cos\phi}{\alpha_p \cos\phi - \omega_0 \sin\phi}\right) - \tan^{-1}\frac{\omega_0}{\alpha_m}, \tag{S22}$$

As described in **Equations 4** and **5** of the main text.

Curve fitting for experimental PRCs

In **Figure 5**, the experimental PRCs for NPY and NMDA were fit to the following function:

$$\Delta\varphi = \varphi - \tan^{-1}\left(\frac{\sin\varphi + rg(\varphi)\sin\theta}{\cos\varphi + rg(\varphi)\cos\theta}\right) \qquad g(\varphi) = \left(1 + e^{-\beta(\cos(\varphi-\varphi_c)+\gamma)}\right)^{-1} \tag{S23}$$

Here, r and θ are the magnitude and direction of perturbation in Glass and Winfree's circular limit cycle model of phase resetting (2), and $g(\varphi)$ is a periodic gating function that controls the circadian times at which the system is sensitive to external perturbation. The parameter β controls the "squareness" of the gating function and φ_c is the phase at the center of the sensitive region (for $\beta > 0$). The sensitive and insensitive phases have equal length if $\gamma = 0$, while the sensitive phase is longer for $\gamma > 0$. For a set of experimentally-observed (φ, $\Delta\varphi$) pairs, optimal values of r, θ, β, φ_c, and γ were found by nonlinear Levenberg-Marquardt fitting.

Exploration of parameter space

The maximum-entropy ensembles described in the "Generation of model ensembles" section of the main text were generated using the following algorithm:

p = initial parameter set (vector with 21 elements)
s = Monte Carlo move size
kT = temperature scale
S() = score function defined in Equations 6-8 of the main text

score = *S*(*p*)
for *i* = 0...200000:
    new_p = *p*
    choose a random integer *j* in [0:21]
    choose a random number *v*, uniformly distributed on (ln(1/*s*):ln(*s*))
    new_p[*j*] = *new_p*[*j*] * exp(*v*)
        new_score = *S*(*new_p*)
    choose a random number *u*, uniformly distributed on (0,1)
    if *(new_score* < *score*) or (exp((*score*-*new_score*)/*kT*) > *u*):
        score = *new_score*
        p = *new_p*
    save *p* for later use

For each sampling temperature *kT* used, the move scale *s* was chosen to give an acceptance rate of ~50%; higher sampling temperatures will require a larger move scale to reach this level. The role of *kT* is essentially to control the algorithm's willingness to go uphill – if *kT* is very small, then exp((*score-new_score*)/*kT*) will tend to be close to zero when *new_score* > *score* and uphill moves will rarely be accepted. If *kT* is large, then exp((*score-new_score*)/*kT*) will often be close to 1 and the algorithm will cheerfully climb hills.

Table S1: Experimentally-derived parameter distributions used for the initial parameter search, as well as the construction of **Figure S2** from **Equations S21** and **S22**. In the initial search, the non-dimensional model parameters were derived from these using **Equations S4** and **S7**, with a characteristic time scale $t_c = 1$. All parameters except the initial distribution of n follow a lognormal distribution with a PDF of

$$\frac{1}{x\sqrt{2\pi\sigma^2}} e^{-\frac{(\ln x-\mu)^2}{2\sigma^2}}.$$

Symbol	Description	PDF
α_m	mRNA degradation rate (h^{-1})	μ=-1.949, σ=0.724
β_m	mRNA transcription rate (nM/h)	μ=-6.608, σ=0.992
n	Hill coefficient	$e^{-(x-1)}$ for $x > 1$
α_p	protein degradation (h^{-1})	μ=-4.199, σ=1.024
β_p	protein translation (h^{-1})	μ=3.519, σ=1.325
k_1	TF-promoter binding constant (nM)	μ=2.0, σ=2.0

Table S2: Model parameters used in **Equation 1** of the main text. The PDFs listed here were calculated from the parameters of the successful oscillators in the initial parameter search. The major difference from the experimentally-derived parameters in **Table S1** is that protein and mRNA decay rates are faster, as would be expected for oscillating transcription factors and their transcripts; see **Figure S1**. The optimized values listed are for the parameter search with probability and knockout constraints ("P" in **Figure 4**).

Parameter	Description	PDF	Optimized value
η_{ma}	mRNA *a* degradation	μ=-1.113, σ=0.805	0.313
η_{mb}	mRNA *b* degradation	μ=-1.113, σ=0.805	1.542
η_{mc}	mRNA *c* degradation	μ=-1.113, σ=0.805	0.551
η_{md}	mRNA *d* degradation	μ=-1.113, σ=0.805	1.157
η_{me}	mRNA *e* degradation	μ=-1.113, σ=0.805	0.267
η_{pA}	protein *A* degradation	μ=-1.006, σ=1.045	0.434
η_{pB}	protein *B* degradation	μ=-1.006, σ=1.045	0.113
η_{pC}	protein *C* degradation	μ=-1.006, σ=1.045	0.328
η_{pD}	protein *D* degradation	μ=-1.006, σ=1.045	0.686
η_{pE}	protein *E* degradation	μ=-1.006, σ=1.045	0.254
n	Hill coefficient	μ=0.693, σ=0.187	3.426
χ_1	repression of *a* by *C*	μ=-5.095, σ=2.610	0.486
χ_2	activation of *b* by *A*	μ=-5.095, σ=2.610	0.731
χ_3	repression of *b* by *E*	μ=-5.095, σ=2.610	6.79×10^{-6}
χ_4	activation of *c* by *A*	μ=-5.095, σ=2.610	0.300
χ_5	activation of *c* by *B*	μ=-5.095, σ=2.610	0.218
χ_6	repression of *c* by *D*	μ=-5.095, σ=2.610	1.384
χ_7	repression of *c* by *E*	μ=-5.095, σ=2.610	6.78×10^{-6}
χ_8	repression of *d* by *C*	μ=-5.095, σ=2.610	0.417
χ_9	activation of *e* by *B*	μ=-5.095, σ=2.610	6.77×10^{-6}
χ_{10}	repression of *e* by *D*	μ=-5.095, σ=2.610	6.70×10^{-6}

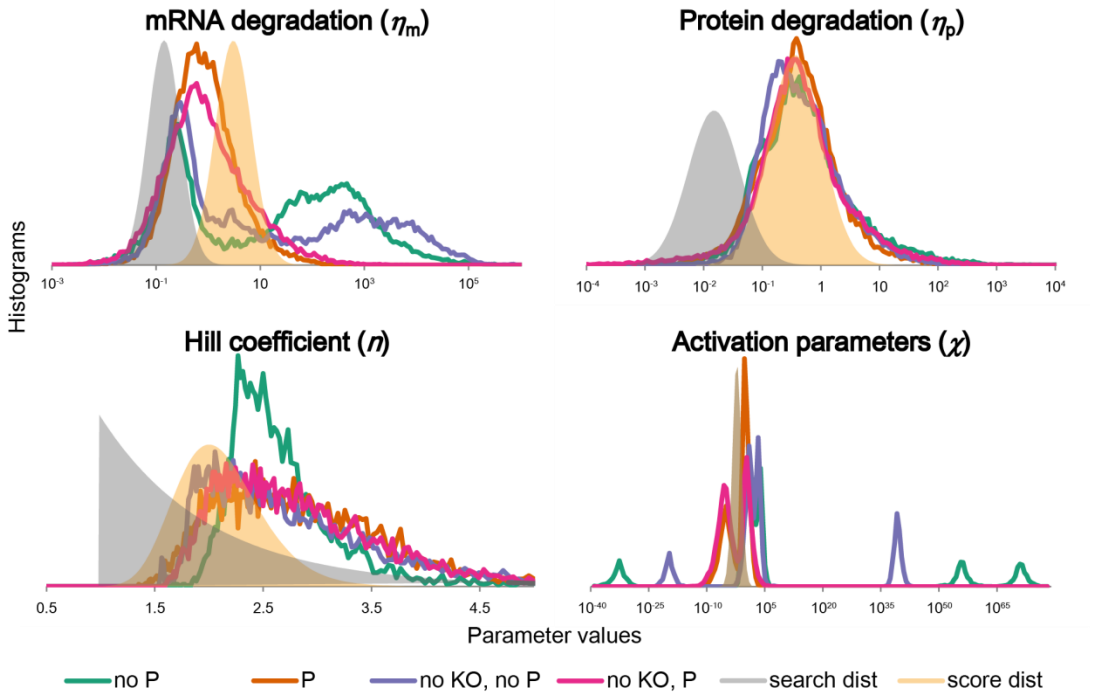

Figure S1: Histograms of parameter values in the ensembles obtained using four different scoring approaches. Naming of the ensembles is as in **Figure 3** of the main text. The shaded "search dist" region shows the experimentally-derived parameter distributions used in the original random search (**Table S1**). Because these distributions were obtained for a broad-based selection of genes and are not specific to oscillating transcription factors, the degradation rates observed in the oscillating sub-population are typically faster than the original distribution. To account for this difference, new probability distributions ("score dist") were inferred from this oscillating sub-population and used for subsequent parameter scoring (**Table S2**).

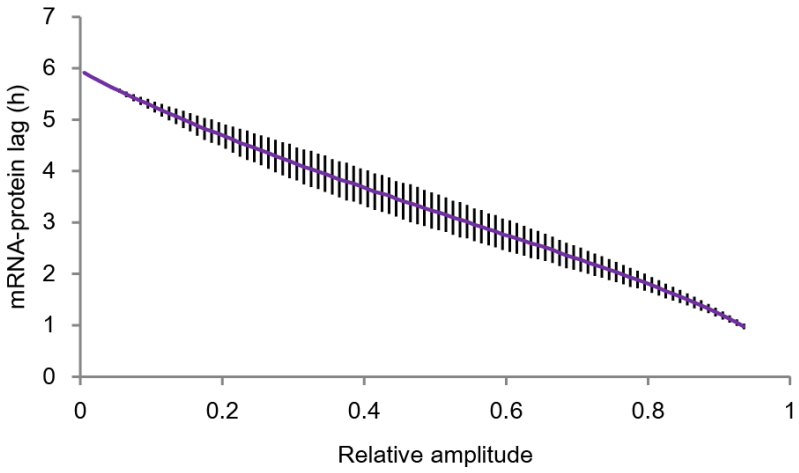

Figure S2: Relationship between relative protein oscillation amplitude and protein-mRNA phase lag. Physically-reasonable values for mRNA and protein degradation rates were drawn from the distributions described in **Table S2** and substituted into **Equations 4** and **5** of the main text to obtain values for the relative protein amplitude and the mRNA-protein phase lag. The nearly-linear relationship between these quantities allows us to infer protein phases based on qPCR measurements of mRNA phase and estimates of protein oscillation amplitude, which are somewhat more reliable than phase estimates.

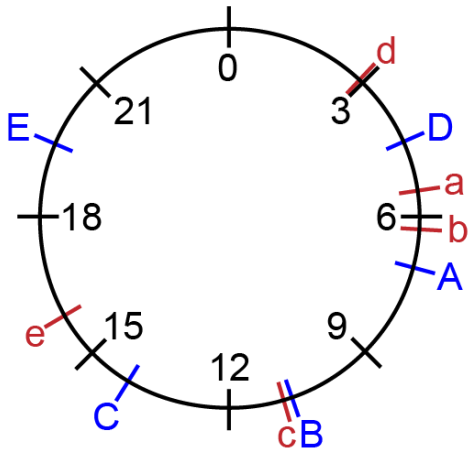

Figure S3: Protein and mRNA phases used in model optimization. Phases of mRNA components were derived from qPCR experiments (see **Figure 2** in the main text), and protein phases were inferred using the linear relationship in **Figure S2**.

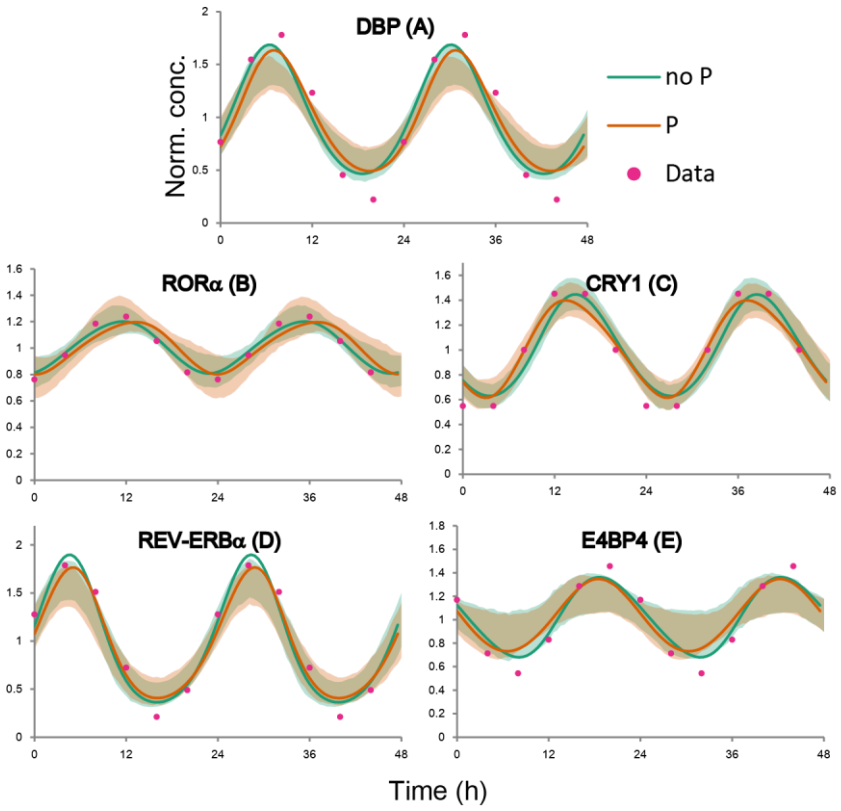

Figure S4: Model outputs for oscillating protein levels, similar to **Figure 2** in the main text. Rather than being directly experimentally-measured, the data points are estimated based on reported protein oscillation amplitudes and phases inferred using **Figure S2**.

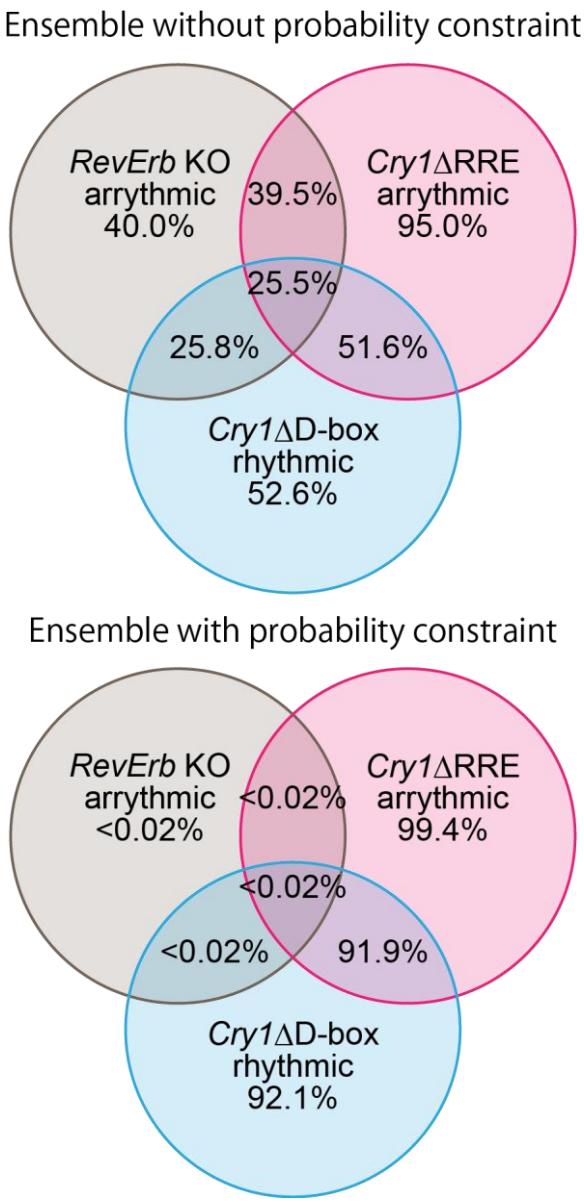

Figure S5: Knockout statistics for the Monte Carlo ensembles in which the knockout constraint was removed. Especially when the probability constraint is used, it appears that the constraints on the regulation of *Cry1* are usually satisfied even if the constraint is not present. The opposite is true for a knockout of the *RevErb* genes; if the constraint is omitted, the correct phenotype is almost never observed. The *RevErb* KO constraint exerted a significant effect on the parameter search and sampling, constraining it to a region of parameter space in which this knockout had an unstable fixed point.

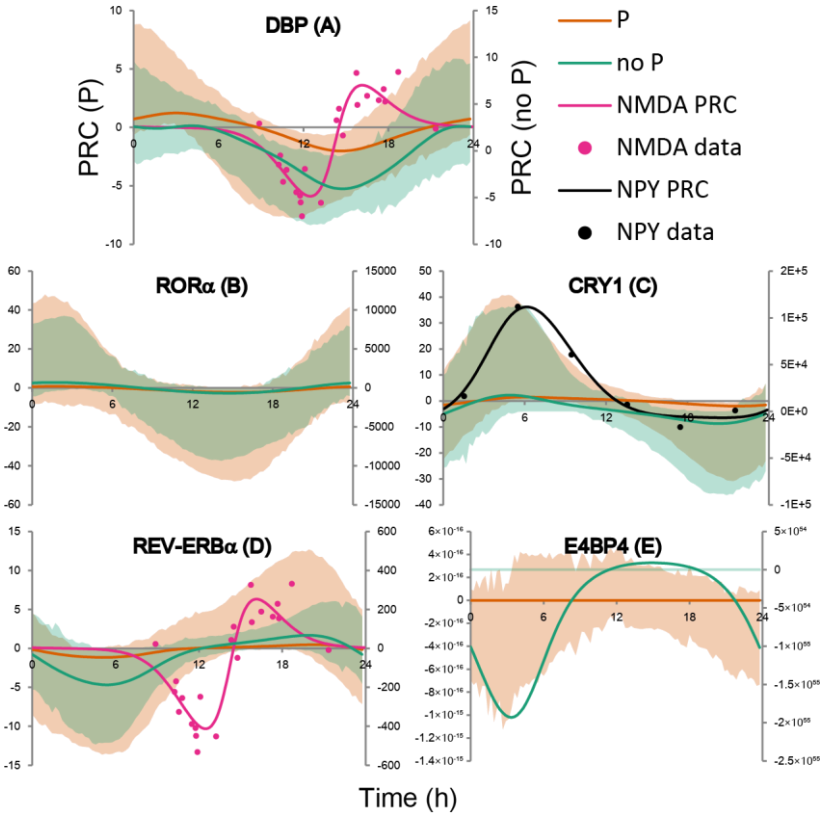

Figure S6: Phase response curves for protein component of the model, similar to Figure 5 in the main text.

References

1. Alon, U. 2007. An introduction to systems biology : design principles of biological circuits. Chapman & Hall/CRC, Boca Raton, FL.
2. Glass, L., and A. T. Winfree. 1984. Discontinuities in phase-resetting experiments. Am J Physiol 246:R251-258.